

Huangyan Li^{ID}, Shi Chen, Filippo Costa^{ID}, Yi Wang^{ID}, Qunsheng Cao^{ID},
Wen Wu^{ID}, and Agostino Monorchio

Simple, Low-Cost, and Reconfigurable Metamaterials and Metasurfaces Based on Reusable Building Blocks

A proposed approach.

A new approach for engineering and fabricating metamaterials and metasurfaces is presented. The design approach is based on reusable building blocks (RBBs) in the form of a stud baseplate and separable RBBs mounted on it. The novelty of the proposed design lies in the reconfigurability of the simple and low-cost structure, which can be easily transformed or modified without a dedicated manufacturing stage. The proposed design approach can be a powerful tool to test experimentally a large number of possible design configurations. A couple of representative examples of the structures comprising nonresonant square and resonant cross elements are presented as a proof of concept based on RBBs. A detailed miniaturization procedure of the cross-plate RBB is then provided to illustrate the versatility of the design approach. To gain a deeper insight into the working mechanism, distributions of the surface current and electric field have also been analyzed. Finally, several

types of RBB prototypes have been fabricated and measured to validate the correctness of the reusable scheme based on RBBs.

INTRODUCTION

Metamaterials are artificially designed compound structures that possess unconventional physical properties that are determined by the structure geometry rather than the material itself [1]. In recent years, metamaterials have had a great impact on a wide range of scientific fields, including electromagnetism, acoustics, mechanics, and thermodynamics. Because of their peculiar electromagnetic (EM) properties, EM metamaterials have been applied in various application areas, such as antenna radomes [2], [3], absorbers [4], [5], and EM compatibility/interference [6], [7].

For many researchers, one common challenging aspect of traditional metamaterials lies in their limited or even fixed frequency characteristics once they are built. Active devices can be loaded to alter the EM properties of metamaterials by regulating the external excitation [8]–[15]. By using some perturbation approaches, the geometric structures of metamaterials

Digital Object Identifier 10.1109/MAP.2021.3110482
Date of current version: 16 September 2021



can be partly or entirely modified so that reconfigurable properties can be attained as the couplings between the incident waves and the conductive structures are changed [16]–[18]. Adaptable materials can also be used as the substrate or part of the structural unit to introduce a reconfigurable capability [19]–[21]. In some practical applications, where it may be necessary to vary the behavior of a frequency-selective structure in two different moments not necessarily close in time, reconfigurable metamaterials with reusability, simple implementation, a low cost, and a short design cycle are in high demand.

In addition, RBBs play a valuable role in the design process of metamaterials. Metamaterial designs first need to be theoretically created and analyzed by using computational EM algorithms. Then, prototypes are fabricated using processing technologies, such as printed circuit board (PCB) machining and 3D printing, before conducting measurements for principle validation. To perform a quick analysis or, alternatively, the final tuning of engineered material properties, which usually requires time-consuming simulations, it is of vital importance to have a platform that allows one to analyze the performance of metamaterials by measurements. This analysis approach would also strengthen engineering education in universities, where students are now encouraged to experience the entire design cycle, including modeling, simulating, analyzing, and measuring. It is much easier for university students to get involved in the theoretical part rather than the experimental process of metamaterial design because fabricating prototypes is expensive and time consuming for large-sized periodic structures using traditional fabrication procedures. In addition, the fabricated samples are not reusable for other students with different design perspectives and parameters [22], which increases the cost and time needed to design metamaterials.

In this article, a useful approach to easily change the shape and thus the response of metamaterials, by simply reallocating RBBs manually, is presented. The proposed design is composed of two separable parts, including RBBs and a stud baseplate on the bottom layer. The RBBs, consisting of conductive patterns and corresponding building blocks, can be replaced by ones with different shapes to achieve reconfigurable characteristics very easily without requiring additional components and corresponding excitation sources. Nonresonant square and resonant cross structures are chosen as RBBs to illustrate the proposed concept. Then, a detailed miniaturization procedure of the cross-plate RBB is presented. Finally, prototypes of different RBBs are fabricated, and the measured results demonstrate the proposed designs, which

Metamaterials are artificially designed compound structures that possess unconventional physical properties that are determined by the structure geometry rather than the material itself.

are characterized by their merits of reusability, easy processing, low cost, and efficient assembly/disassembly. The approach based on RBBs opens up a new perspective on engineering metamaterials. It could be a convenient tool for testing many representative meta-material configurations without the need for a costly and time-consuming fabrication procedure based on photolithography. Moreover, it could be a useful tool for experimental teaching in colleges and universities.

THE FABRICATION APPROACH

The proposed metamaterials based on RBBs are composed of two detachable parts: a stud baseplate and the RBBs built on it. The stud baseplate and its geometrical parameters are denoted in Figure 1, where u is the periodicity of each unit cell, and rad_1

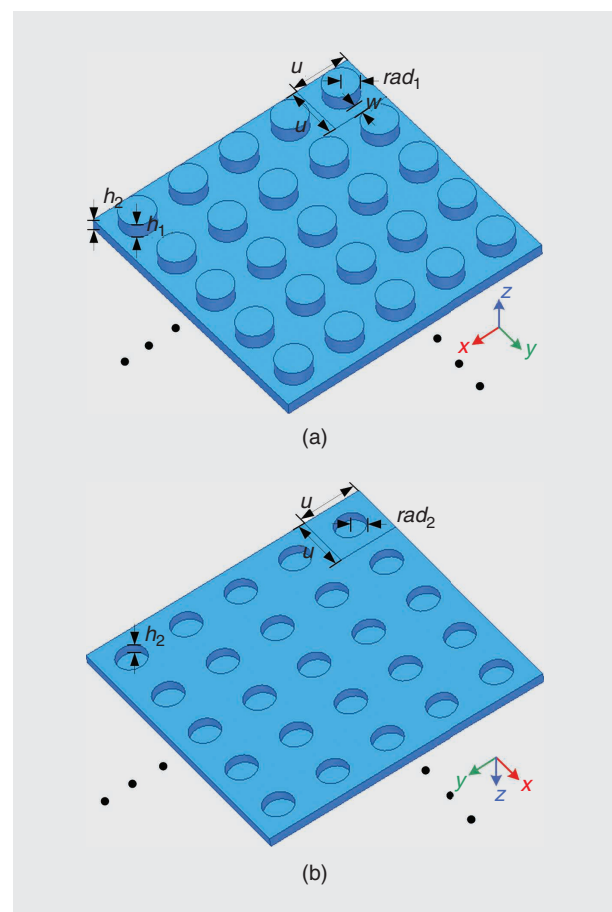


FIGURE 1. A sketch diagram of the stud baseplate. (a) Front side. (b) Back side. Detailed geometrical parameters are $u = 7.8 \text{ mm}$, $rad_1 = 2.4 \text{ mm}$, $rad_2 = 2 \text{ mm}$, $w = 1.5 \text{ mm}$, $h_1 = 1.7 \text{ mm}$, and $h_2 = 1.3 \text{ mm}$.



FIGURE 2. Representative realizable shapes based on basic RBBs.

and rad_2 are the radii of the external studs and internal cylindrical grooves, respectively. The straight-line distance between two adjacent studs is represented by $2w$, and w satisfies the relation $w = (u - 2rad_1)/2$. The heights of the studs and the baseplate are h_1 and h_2 , respectively. The baseplate is constructed of acrylonitrile butadiene styrene (ABS), which is regarded as the workhorse of plastics because of its durability, low cost, and process controllability. The studs are evenly distributed on the

baseplate for the convenience of perfectly combining the baseplate with the RBBs, whose main bodies are also made of ABS materials and can be designed into various shapes based on basic RBBs that already exist.

Some representative examples of the realizable unit cell shapes based on the proposed approach are shown in Figure 2. The diameter of the stud and the gap between two adjacent ones should be considered for designing the stud baseplate

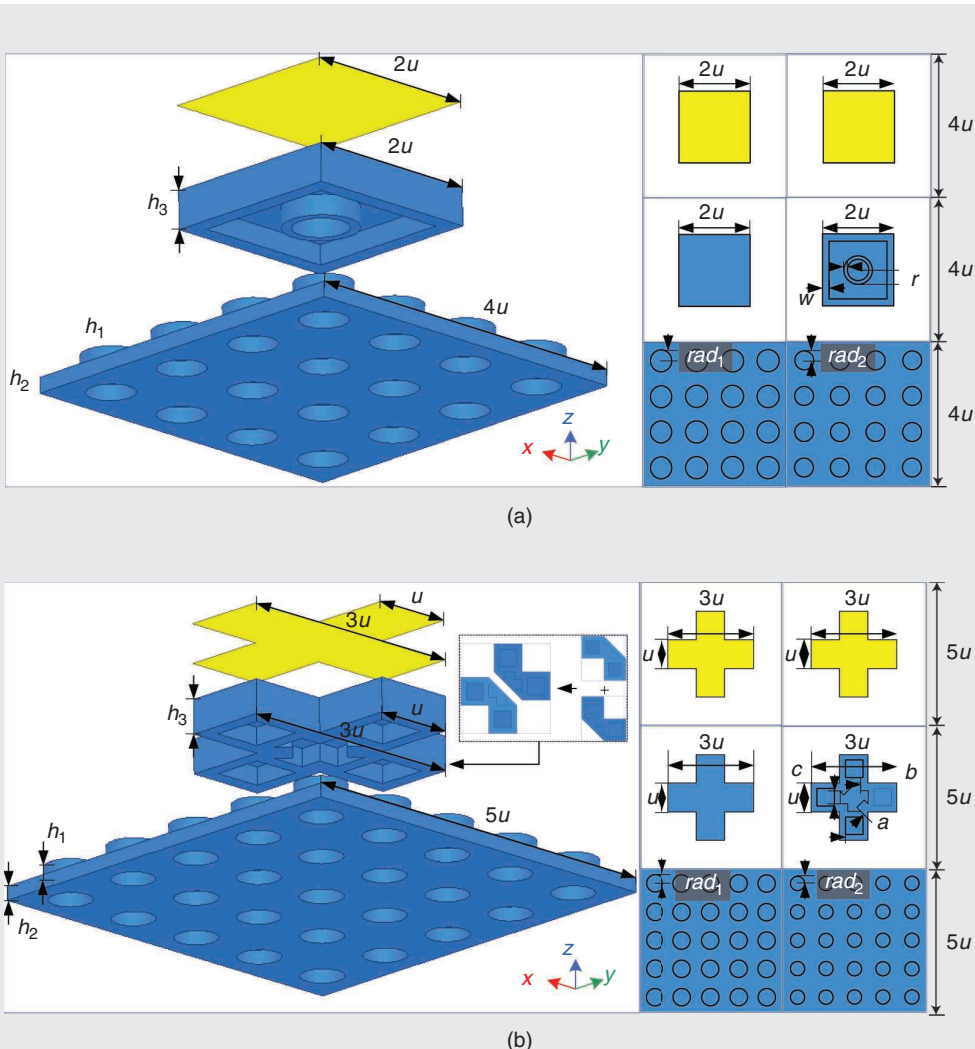


FIGURE 3. The structural elements of the metamaterial based on different RBBs. (a) Square-plate RBB. (b) Cross-plate RBB. Detailed geometrical parameters are $r \approx 3.12$ mm, $r_w = 0.8$ mm for the square-plate RBB; $a = 3$ mm, $b \approx 2.20$ mm, $c \approx 3.48$ mm, and $n = 4.8$ mm for the cross-plate RBB; $h_3 = 3.2$ mm for both RBBs.

since the assembly and geometric parameters of RBBs mainly depend on the studs. Adhesive copper foil tapes are used to implement conductive surfaces in the following design examples as they are cost-effective and readily available in the laboratory. However, other metallic materials (e.g., copper, silver, and aluminum) can also be employed to realize conductive RBB surfaces with only slight variations in the magnitude of the scattering parameters. It is well known that the EM characteristics (e.g., the resonant frequency and bandwidth) of the overall structure are mainly influenced by the substrate (the dielectric constant and the thickness) and the metallic pattern (the geometric parameters). Thus, 3D printing technology can be utilized to realize the desired baseplate and building blocks, where different substrate materials can be chosen and various complex shapes can be custom made in one step according to different requirements.

To show the potentialities of the proposed method, two simple examples of planar periodic structures (periodic arrays of patches and crosses) are presented in the next section. Moreover, an approach to transform the structure into a 3D miniaturized structure is proposed. Following a similar approach, many other 2D or 3D periodic or nonperiodic structures can be fabricated. The designed surfaces are also manufactured and tested to verify their performance.

DESIGN EXAMPLES

Some specific examples are discussed in this section. Initially, two examples of planar periodic structures, i.e., metasurfaces, are discussed. Then, an approach for the miniaturization of the cross structure based on a 3D structure is presented. By extending the proposed fabrication approach and stacking additional layers, even more complicated designs could be obtained.

PLANAR STRUCTURES: SQUARE-PLATE AND CROSS-PLATE RBBs

The structural elements of the metamaterials based on the square-plate and the cross-plate RBBs are shown in Figure 3(a) and (b), respectively. The RBB in Figure 3(a) is a 2×2 square plate, whose upper surface is covered by a conductive square pattern. A hollow cylinder together with the inner structure of the square-plate RBB is intended to fit tightly with four studs on the baseplate. The cross-plate RBB in Figure 3(b) is formed by two 2×2 cut-corner plates, and a cross metal sheet covers its top surface. One windmill- and four square-type grooves are used in the cross-plate RBB to ensure a very tight contact with the five studs of the

stud baseplate. The geometrical parameters of the square-plate and the cross-plate RBBs are also given in Figure 3, and they have the same thickness $h_3 = (u - 2rad_1)/2 + h_1$. In addition, r and r_w are the external radius and the thickness of the hollow cylinder of the square-plate RBB, respectively, and r

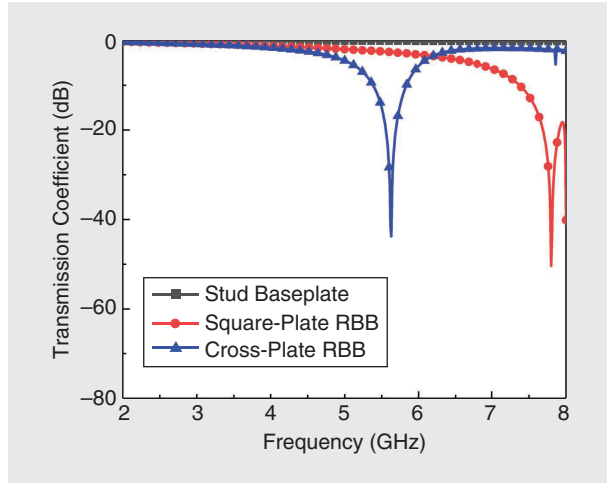


FIGURE 4. The simulated transmission coefficients of the metamaterial based on different RBBs.

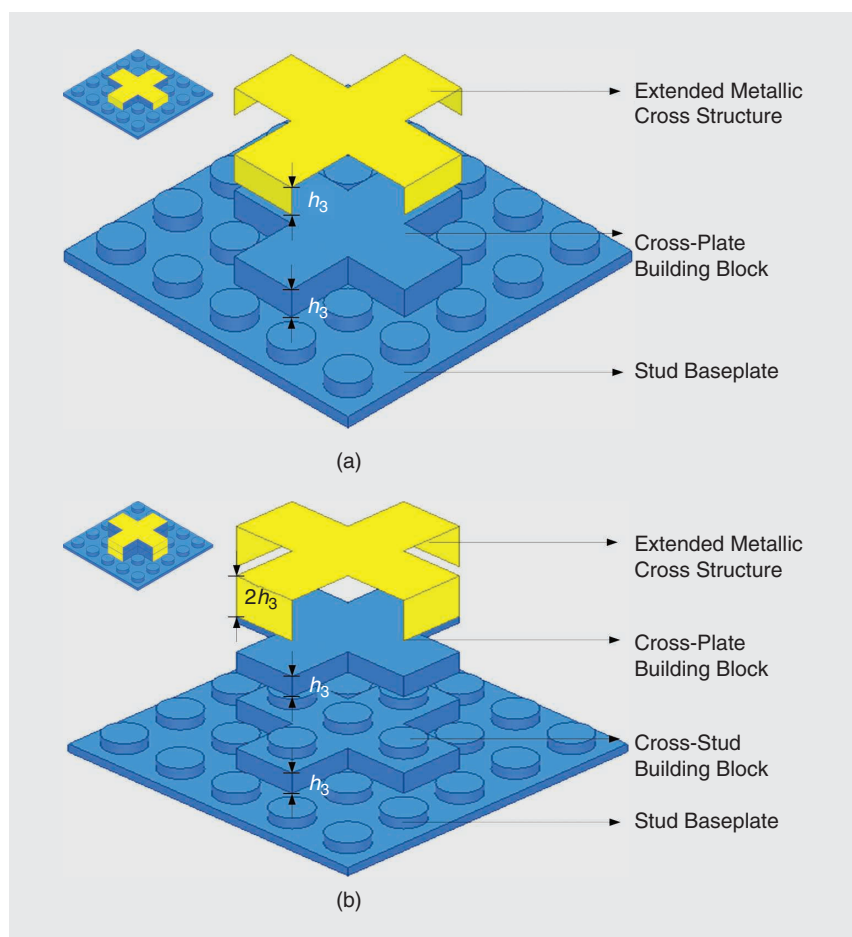


FIGURE 5. The miniaturization evolutionary process of the metamaterial based on the miniaturized cross RBBs. (a) Intermediate cross-plate RBB. (b) Miniaturized cross RBB.

can be computed by $r = (\sqrt{2}u - 2rad_1)/2$. The parameters that describe the windmill- and square-type grooves of the cross-plate RBB are as follows: $a = 2w$, $b = (u - \sqrt{2}rad_1)/2$, $c = u - b - \sqrt{2}w$, $n = u - 2w$.

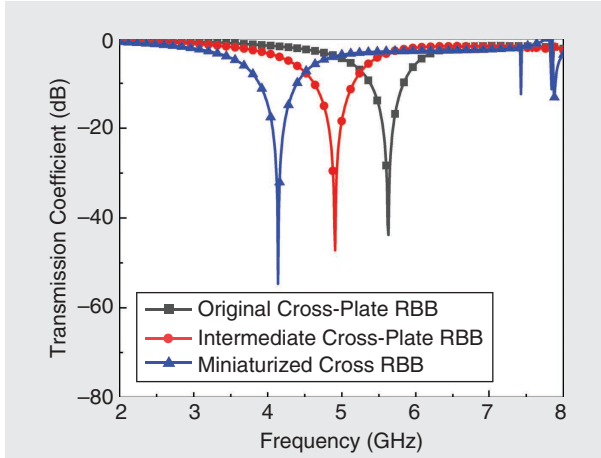


FIGURE 6. The simulated transmission coefficients of the miniaturized metamaterial based on the miniaturized cross RBBs.

To verify the validity of the concept, a full-wave high-frequency structure simulator is employed to compute the transmission coefficients of the combined structures. Two pairs of master-slave boundaries are applied to four faces of the structure to mimic the periodic extension along the x - and y -axes, and a pair of Floquet excitations is assigned to both the top and bottom sides along the z -axis. The simulated transmission performance of the metamaterial based on the RBBs is plotted in Figure 4. There is almost no reflection when no RBB is built on the stud baseplate because of the lack of metallic structures; thus, the incident waves transmit through the stud baseplate. After assembling nonresonant square-plate RBBs on the stud baseplate, low-pass filtering characteristics can be obtained. A stopband is produced with an operating frequency at 5.63 GHz when resonant cross-plate RBBs are utilized. Therefore, a simple, low-cost and reusable metamaterial can be easily realized by adopting different RBBs.

3D STRUCTURES: MINIATURIZATION OF THE CROSS-PLATE RBB

This section presents the miniaturization strategy for the RBBs based on the cross-type element. The element shown in Figure 3(b) can be miniaturized by introducing large face couplings

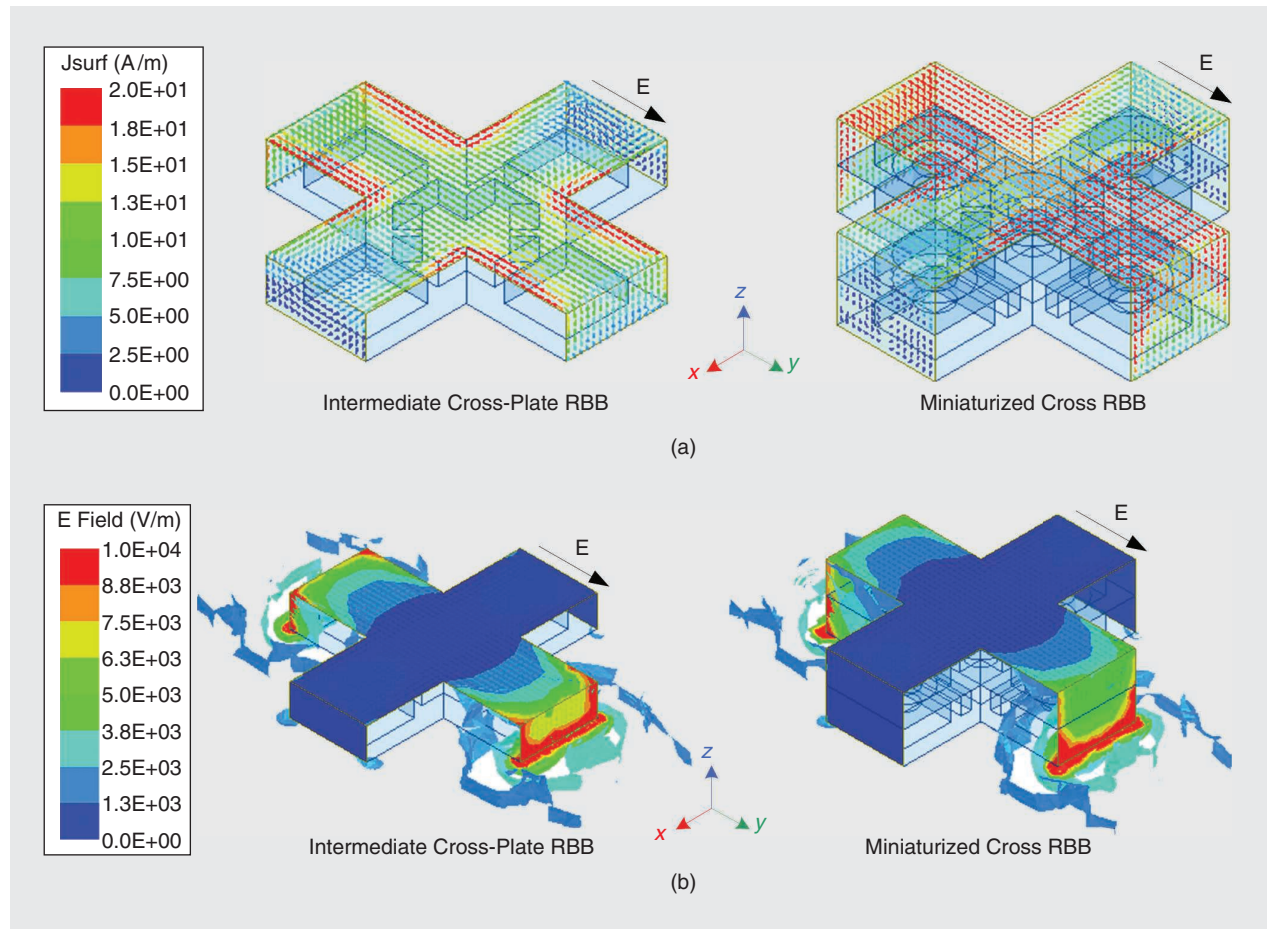


FIGURE 7. The surface current and electric field distributions of the modified cross-plate RBBs. (a) Surface current. (b) Electric field.

to replace the former edge couplings, which greatly enhances the equivalent capacitance. Thus, the resonant frequency can be reduced at a fixed element dimension. The lower the resonant

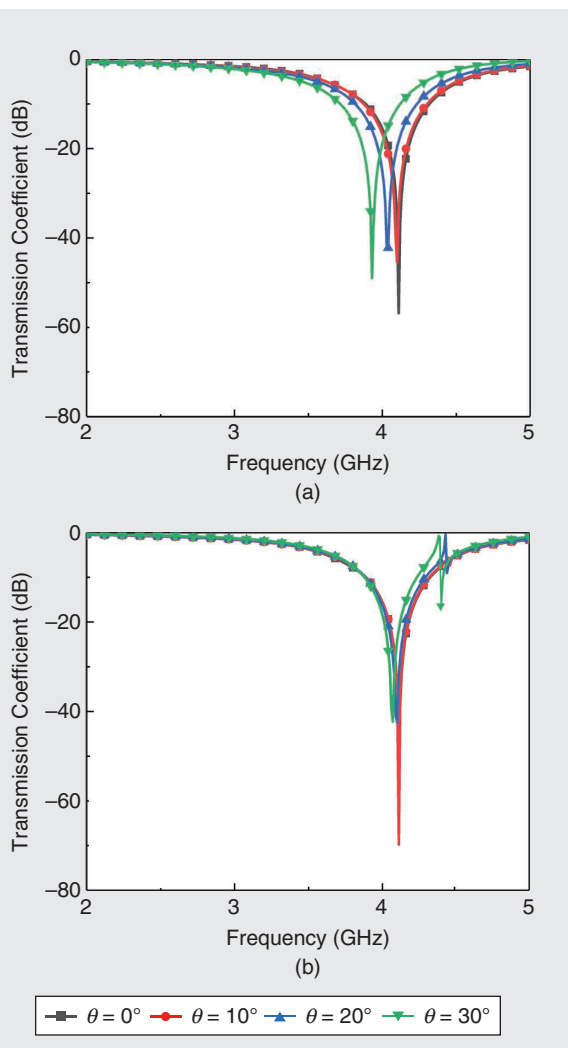


FIGURE 8. The simulated transmission coefficients of the metamaterial based on the miniaturized cross RBBs under oblique incidence. (a) TE polarization. (b) TM polarization. TE: transverse electric; TM: transverse magnetic.

frequency, the higher the miniaturization level that can be realized. As shown in Figure 5(a), the length of the metallic cross structure in Figure 3(b) is extended by h_3 to cover the four

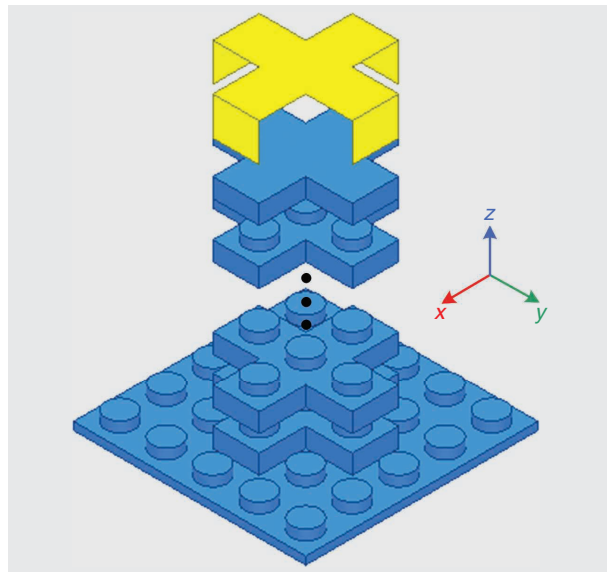


FIGURE 9. Further miniaturization of the miniaturized cross RBB.

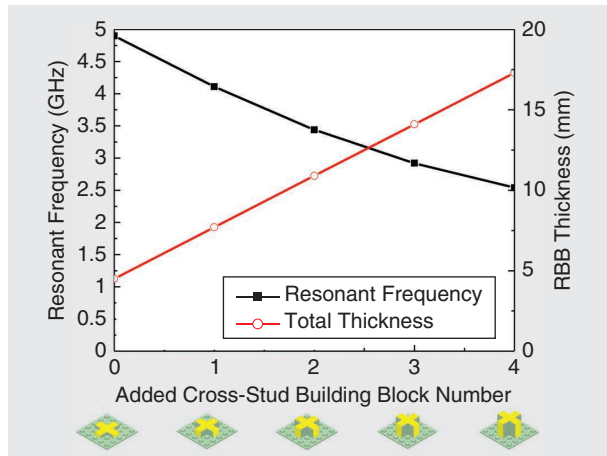


FIGURE 10. The compromise between miniaturization level and total thickness of the miniaturized cross RBB when the number of cross-stud building blocks changes.

TABLE 1. THE ANGLE STABILITY VALUES OF THE REUSABLE METAMATERIALS BASED ON MINIATURIZED CROSS RBBS WITH DIFFERENT MINIATURIZATION LEVELS.

Number of Added Cross-Stud Building Blocks	Thickness (mm)	Center Frequency Shift (%)							
		TE mode				TM mode			
		15°	30°	45°	60°	15°	30°	45°	60°
0	4.5	2.65	9.39	15.92	20.61	0	1.43	9.39	13.88
1	7.7	0.97	4.38	7.79	11.44	0	0.97	3.16	6.33
2	10.9	0.58	1.74	3.49	5.52	0.29	0.87	1.74	3.77
3	14.1	0.34	0.68	1.71	2.74	0	0.34	1.03	3.08
4	17.3	0	1.18	1.18	1.97	0	0.79	1.18	2.36

sides of the cross-plate building block. In Figure 5(b), an extra cross-stud building block is assembled between the stud base-plate and the cross-plate building block. In this way, the extended length can be further increased by using the space region. The simulated transmission performance of the metamaterial based on the miniaturized cross RBBs is plotted in Figure 6. As can be observed, the resonant frequencies of the metamaterials based on the original cross-plate RBBs, intermediate cross-plate RBBs, and miniaturized cross RBBs are 5.63 GHz, 4.90 GHz, and 4.11 GHz, respectively.

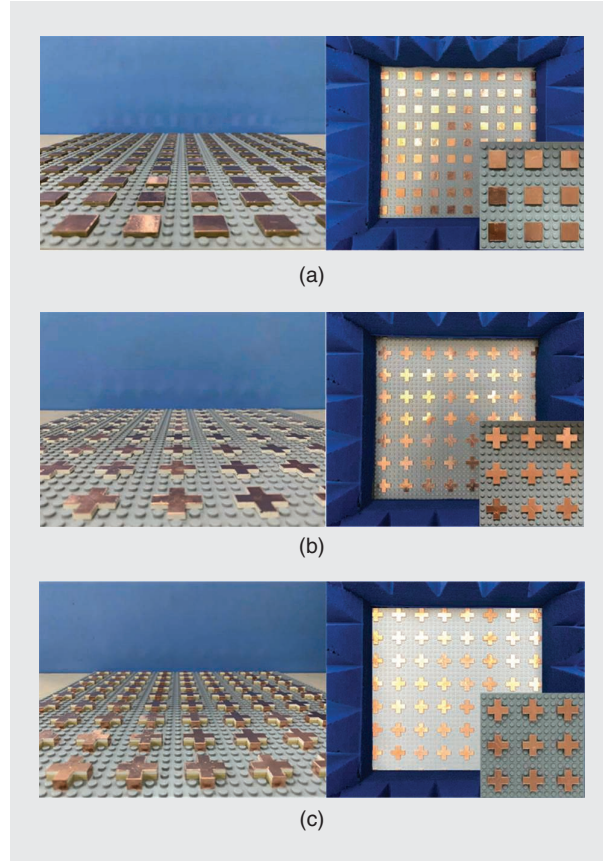


FIGURE 11. Prototypes of the metamaterial based on different RBBs. (a) Square-plate RBB. (b) Cross-plate RBB. (c) Miniaturized cross RBB.

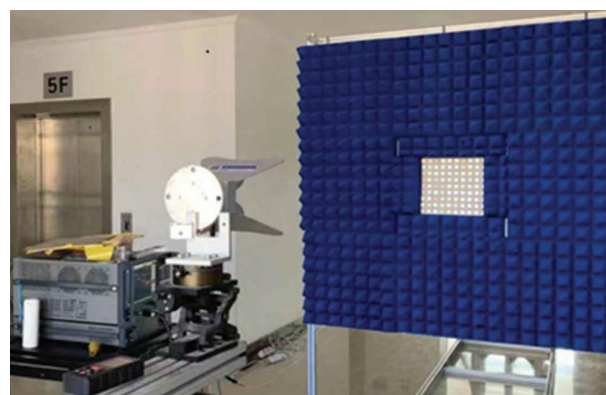
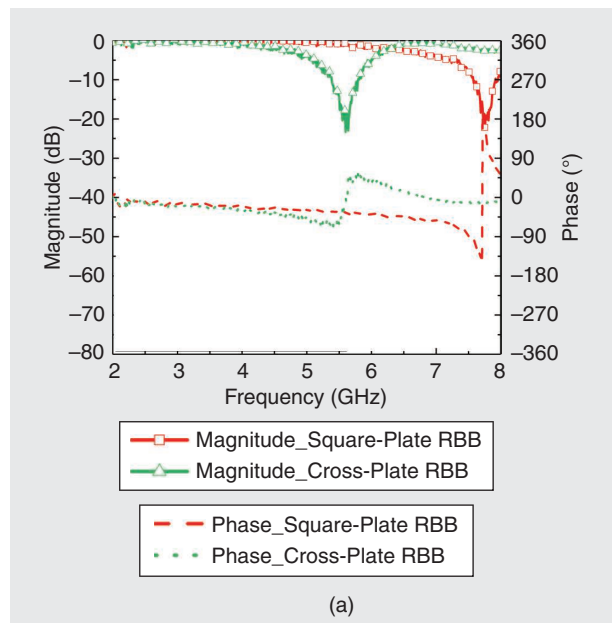


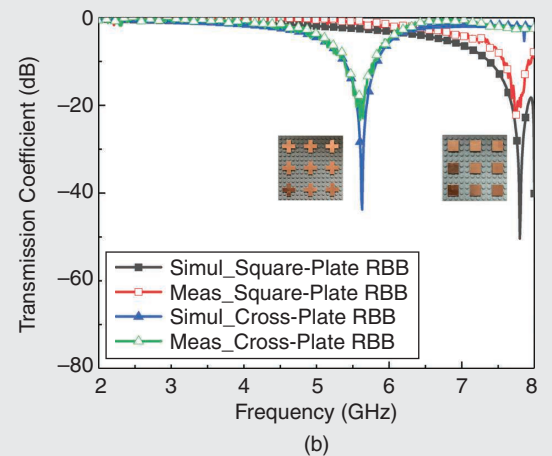
FIGURE 12. The measurement setup.

To better understand the miniaturization mechanism of the miniaturized cross RBBs, distributions of the surface current and electric field are presented in Figure 7. As can be observed, the equivalent inductance increases moderately as the equivalent resonance length is elongated, and meanwhile, the equivalent capacitance is greatly enhanced because of the large face couplings produced by the parallel overlapping metallic sheets between adjacent elements. Therefore, the resonant frequency of the metamaterial based on the miniaturized cross RBBs can be reduced as the unit cell dimension remains unchanged, leading to an increase of the miniaturization level.

The simulated results of the metamaterial, when assembled with the miniaturized cross RBBs, under different polarizations and incidence angles are plotted in Figure 8. The responses at transverse magnetic (TM) mode are more stable than those at



(a)



(b)

FIGURE 13. The measured transmission results of the metamaterial based on the square-plate and cross-plate RBBs. (a) Magnitudes and phases. (b) Comparison between measurement and simulation results.

transverse electric (TE) mode since slight frequency shifts can be observed as the incident angle increases.

The size of the miniaturized cross RBB can be further reduced by adding more pieces of cross-stud building blocks between the stud baseplate and the metallized cross-plate building block, as shown in Figure 9. However, note that there exists a compromise between the miniaturization level and the overall structural thickness. As depicted in Figure 10, the resonant frequency can be greatly reduced at a given structural size, while the total thickness of the RBB increases simultaneously as more cross-stud building blocks are added. The angle stabilities of the metamaterials based on different miniaturized cross RBBs are summarized in Table 1. As the number of added cross-stud building blocks increases, the performance with respect to different incident angles becomes more stable.

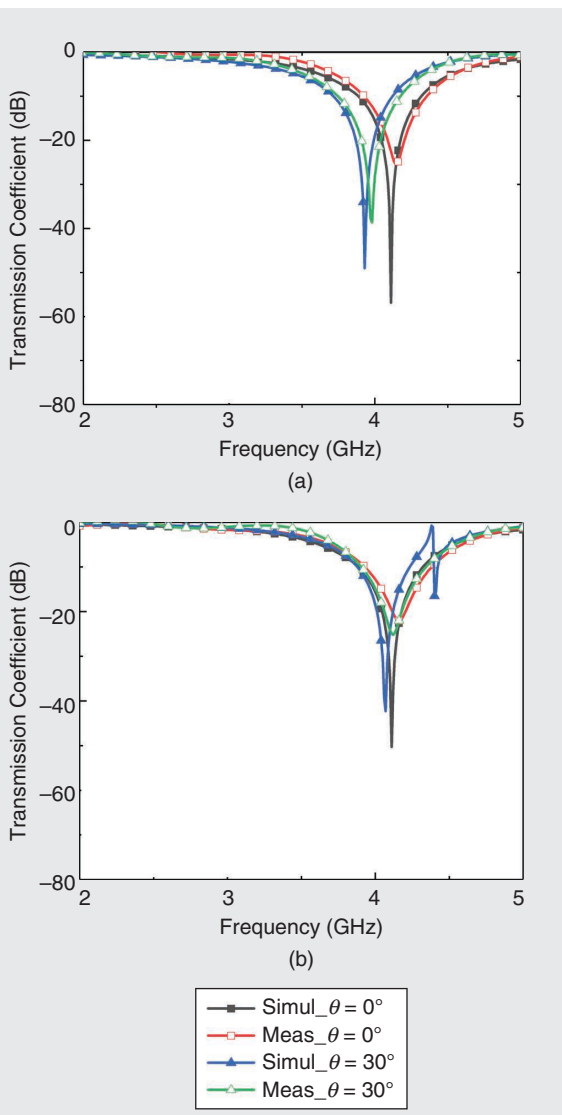


FIGURE 14. The measured and simulated transmission results of the metamaterial based on the miniaturized cross RBBs under oblique incidence. (a) TE mode. (b) TM mode.

EXPERIMENTAL RESULTS

To validate the simulation results, some prototypes of the metamaterials based on different types of RBBs are fabricated, as shown in Figure 11. A gray-colored 48×48 -stud baseplate with an overall physical dimension of $380 \text{ mm} \times 380 \text{ mm}$ is chosen in the experiment. A 2×2 square plate is employed as the building block of the square-plate RBB, and two 2×2 cut-corner plates are combined to form a cross-plate RBB. The miniaturized cross RBB containing one added 3×3 cross-stud building block is fabricated as an illustration to demonstrate the miniaturized design. To achieve conduction characteristics, the top surfaces of the building blocks are covered by 0.065-mm-thick adhesive copper foil tape.

The free-space method is used for the measurements. As shown in Figure 12, the measurement setup includes a pair of horn antennas (1–18 GHz) with one working as the transmitter and another as the receiver; both are connected by an Agilent N5245A vector network analyzer. In addition, the prototypes under test are surrounded by a large custom-built absorbing frame to reduce the edge diffraction. The measurement process includes two steps. First, the transmission properties without the prototype are measured. Then, the experimental results with the prototype are obtained and normalized to the ones in the first step.

The measured magnitudes and phases of the metamaterials based on the square-plate and cross-plate RBBs are presented in Figure 13(a), and the transmission results are compared with the simulated ones in Figure 13(b). The structure works as a low-pass filter once nonresonant square-plate RBBs are built on the stud baseplate, and a stopband can be observed at 5.6 GHz when the square-plate RBBs are removed and replaced with cross-plate RBBs. The measured transmission performance of the metamaterial based on the miniaturized cross RBBs is shown in Figure 14. It can be observed that the center frequency of the stopband decreases from 5.6 GHz to 4.15 GHz under normal incidence because of the miniaturization technique. The situation of oblique incidence is also considered and measured. In addition, the measured results are compared with the simulated ones, and they agree very well with each other, demonstrating the design concept of the proposed structure.

CONCLUSIONS

This article explores the potentiality of employing RBBs to achieve metamaterials that enable easy reconfiguration and prototype design. Square-plate, cross-plate, and miniaturized cross RBBs have been designed, fabricated, installed, and validated through numerical and experimental results. The proposed concept uses various RBBs to realize reconfigurable characteristics, and all constituent parts of the proposed designs are very low in cost and easy to operate compared to those in a traditional PCB production process. The RBBs are also reusable once built, and a reconfigurable performance can be attained by simply choosing different RBBs. In addition, all RBBs can be demounted, collected, and utilized for later experiments. By virtue of these features, a metamaterial based on RBBs also serves as a good candidate for purposes of student teaching and research design, where experiment resources and budgets are limited. In addition, the

proposed concept can be easily extended to design structures with many other EM performance aspects, such as beam tilting, polarization selection, and high-order filtering.

ACKNOWLEDGMENTS

This work was supported by the Natural Science Foundation of China under grant 61871219, the Key Laboratory of Radar Imaging and Microwave Photonics (Nanjing University of Aeronautics and Astronautics), and the Ministry of Education, under grant NJ20210002.

AUTHOR INFORMATION

Huangyan Li (huangyan_lee@163.com) is currently a lecturer at Nanjing University of Science and Technology, Nanjing, 210094, China. His research interests include frequency-selective surfaces (FSSs), especially multifunctional and optically controlled reconfigurable FSSs. He is a Member of IEEE.

Shi Chen (chenshi@nuaa.edu.cn) is currently a graduate student at Nanjing University of Aeronautics and Astronautics, Nanjing, 210016, China. Her research interests include generalized sheet transition conditions (GSTCs), especially the analysis of frequency-selective surfaces by GSTCs.

Filippo Costa (filippo.costa@iet.unipi.it) is currently an assistant professor at the University of Pisa, Pisa, 56122, Italy. His research interests include metamaterials, metasurfaces, antennas, and radio-frequency identification. He is a Senior Member of IEEE.

Yi Wang (jflsjfls@nuaa.edu.cn) is currently an associate professor at Nanjing University of Aeronautics and Astronautics, Nanjing, 210016, China. His research interests include finite-difference time-domain (FDTD) modeling of the entire Earth-ionosphere system, earthquake electromagnetics, and FDTD simulation of anisotropic media and earthquake phenomena. He is a Member of IEEE.

Qunsheng Cao (qunsheng@nuaa.edu.cn) is currently a professor at Nanjing University of Aeronautics and Astronautics, Nanjing, 210016, China. His research interests include computational electromagnetics, antennas, radar signal processing, and high-speed circuit signal integrity.

Wen Wu (wuwen@mail.njust.edu.cn) is currently a professor at Nanjing University of Science and Technology, Nanjing, 210094, China. His research interests include microwave and millimeter-wave theories and technologies, microwave and millimeter-wave detection, and multimode compound detection. He is a Senior Member of IEEE.

Agostino Monorchio (a.monorchio@iet.unipi.it) is currently a professor at the University of Pisa, Pisa, 56122, Italy. His research interests include computational electromagnetics, microwave metamaterials, radio propagation for wireless systems, antenna designs, electromagnetic compatibility, and biomedical microwave applications. He is a Fellow of IEEE.

REFERENCES

- [1] M. Kadic, T. Bückmann, R. Schittny, and M. Wegener, "Metamaterials beyond electromagnetism," *Rep. Progr. Phys.*, vol. 76, no. 12, p. 126501, Nov. 2013. doi: 10.1088/0034-4885/76/12/126501.
- [2] J. Kim, H. Chun, I. Hong, Y. Kim, and Y. Park, "Analysis of FSS radomes based on physical optics method and ray tracing technique," *IEEE Antennas Wireless Propag. Lett.*, vol. 13, pp. 868–871, May 2014. doi: 10.1109/LAWP.2014.2320978.
- [3] Y. Shang, Z. Shen, and S. Xiao, "Frequency-selective absorber based on square-loop and cross-dipole arrays," *IEEE Trans. Antennas Propag.*, vol. 62, no. 11, pp. 5581–5589, Nov. 2014. doi: 10.1109/TAP.2014.2357427.
- [4] T. Liu, X. Cao, J. Gao, Q. Zheng, W. Li, and H. Yang, "RCS reduction of waveguide slot antenna with metamaterial absorber," *IEEE Trans. Antennas Propag.*, vol. 61, no. 3, pp. 1479–1484, Mar. 2013. doi: 10.1109/TAP.2012.2231922.
- [5] M. Yoo and S. Lim, "Polarization-independent and ultrawideband metamaterial absorber using a hexagonal artificial impedance surface and a resistor-capacitor layer," *IEEE Trans. Antennas Propag.*, vol. 62, no. 5, pp. 2652–2658, May 2014. doi: 10.1109/TAP.2014.2308511.
- [6] L. Zhang, G. Yang, Q. Wu, and J. Hua, "A novel active frequency selective surface with wideband tuning range for EMC purpose," *IEEE Trans. Magn.*, vol. 48, no. 11, pp. 4534–4537, Nov. 2012. doi: 10.1109/TMAG.2012.2202099.
- [7] I. Syed, Y. Ranga, L. Matekovits, K. Esselle, and S. Hay, "A single-layer frequency-selective surface for ultrawideband electromagnetic shielding," *IEEE Trans. Electromagn. Compat.*, vol. 56, no. 6, pp. 1404–1411, Dec. 2014. doi: 10.1109/TEMC.2014.2316288.
- [8] P. Taylor, E. Parker, and J. Batchelor, "An active annular ring frequency selective surface," *IEEE Trans. Antennas Propag.*, vol. 59, no. 9, pp. 3265–3271, Sept. 2011. doi: 10.1109/TAP.2011.2161555.
- [9] H. Li, Q. Cao, and Y. Wang, "A novel 2-B multifunctional active frequency selective surface for LTE-2.1 GHz," *IEEE Trans. Antennas Propag.*, vol. 65, no. 6, pp. 3084–3092, June 2017. doi: 10.1109/TAP.2017.2688927.
- [10] H. Li, Q. Cao, L. Liu, and Y. Wang, "An improved multifunctional active frequency selective surface," *IEEE Trans. Antennas Propag.*, vol. 66, no. 4, pp. 1854–1862, Apr. 2018. doi: 10.1109/TAP.2018.2800727.
- [11] F. Costa, A. Monorchio, and G. Vastante, "Tunable high-impedance surface with a reduced number of varactors," *IEEE Antennas Wireless Propag. Lett.*, vol. 10, pp. 11–13, Jan. 2011. doi: 10.1109/LAWP.2011.2107723.
- [12] F. Bayatpur and K. Sarabandi, "Design and analysis of a tunable miniaturized-element frequency-selective surface without bias network," *IEEE Trans. Antennas Propag.*, vol. 58, no. 4, pp. 1214–1219, Apr. 2010. doi: 10.1109/ICMTCE.2011.5915165.
- [13] A. Ebrahimi, Z. Shen, W. Withayachumrakul, S. F. Al-Sarawi, and D. Abbott, "Varactor-tunable second-order bandpass frequency-selective surface with embedded bias network," *IEEE Trans. Antennas Propag.*, vol. 64, no. 5, pp. 1672–1680, May 2016. doi: 10.1109/TAP.2016.2537378.
- [14] F. Deng, X. Xi, J. Li, and F. Ding, "A method of designing a field controlled active frequency selective surface," *IEEE Antennas Wireless Propag. Lett.*, vol. 14, pp. 630–633, Dec. 2015. doi: 10.1109/LAWP.2014.2375376.
- [15] X. Su et al., "Active metasurface terahertz deflector with phase discontinuities," *Opt. Express*, vol. 23, no. 21, pp. 27,152–27,158, Oct. 2015. doi: 10.1364/OE.23.027152.
- [16] K. Fuchi, J. Tang, B. Crowgey, A. Diaz, E. Rothwell, and R. Ouedraogo, "Origami tunable frequency selective surfaces," *IEEE Antennas Wireless Propag. Lett.*, vol. 11, no. 6, pp. 473–475, Apr. 2015. doi: 10.1109/LAWP.2012.2196489.
- [17] M. Li, B. Yu, and N. Behdad, "Liquid-tunable frequency selective surfaces," *IEEE Microw. Wireless Compon. Lett.*, vol. 20, no. 8, pp. 423–425, Aug. 2010. doi: 10.1109/LMWC.2010.2049257.
- [18] X. Chen, J. Gao, C. Fang, N. Xu, Y. Wang, and Y. Tang, "Deformable frequency selective surface structure with tuning capability through thermoregulating," *Opt. Express*, vol. 23, no. 12, pp. 16,329–16,338, June 2015. doi: 10.1364/OE.23.016329.
- [19] M. Gil et al., "Electrically tunable splitting resonators at microwave frequencies based on bariumstrontium-titanate thick films," *Electron. Lett.*, vol. 45, no. 8, pp. 417–418, Apr. 2009. doi: 10.1049/el.2009.3055.
- [20] L. Kang, Q. Zhao, H. Zhao, and J. Zhou, "Magnetically tunable negative permeability metamaterial composed by split ring resonators and ferrite rods," *Opt. Express*, vol. 16, no. 12, pp. 8825–8834, June 2008. doi: 10.1364/OE.16.008825.
- [21] Y. Zhang, Y. Feng, B. Zhu, J. Zhao, and T. Jiang, "Graphene based tunable metamaterial absorber and polarization modulation in terahertz frequency," *Opt. Express*, vol. 22, no. 19, pp. 22,743–22,752, Sept. 2014. doi: 10.1364/OE.22.022743.
- [22] U. Bulus, "Anten'it: A hardware-based antenna design and training kit [Testing Ourselves]," *IEEE Antennas Propag. Mag.*, vol. 62, no. 1, pp. 107–112, Feb. 2020. doi: 10.1109/MAP.2019.2955827.

